Journal of Sustainable Development; Vol. 7, No. 2; 2014
ISSN 1913-9063 E-ISSN 1913-9071
Published by Canadian Center of Science and Education

# The Method Estimating Daytime $CO_2$ Flux Between Intertidal Sediment and the Atmosphere

Pengjin Yang[1,2] & Longjun Zhang[2]

[1] North China Sea Environmental Monitoring Center, State Oceanic Administration, Qingdao, China

[2] Key Lab of Marine Environmental Science and Ecology, Ministry of Education, Ocean University of China (OUC), Qingdao, China

Correspondence: Pengjin Yang, North China Sea Environmental Monitoring Center, State Oceanic Administration, Qingdao, China. E-mail: pengjin.7777@163.com

Received: November 11, 2013 Accepted: December 9, 2013 Online Published: March 12, 2014

doi:10.5539/jsd.v7n2p105 URL: http://dx.doi.org/10.5539/jsd.v7n2p105

**Abstract**

The daytime variation in $CO_2$ flux between the intertidal sediment and the atmosphere was great and impacted by environmental elements. This paper analyzed the daytime variation in $CO_2$ flux between the intertidal sediment and the atmosphere and concluded its different rules during the ebb tide and flood tide. During the ebb tide, the $CO_2$ flux rose as the tide ebbed and its rate of change was different when the redox potential changed (0.13 μmol $m^{-2}$ $s^{-1}$ per 100 cm height of the tide at Eh ≤ 300 mv, 0.15 μmol $m^{-2}$ $s^{-1}$ per 100 cm height of the tide at 300 mv < Eh < 500 mv and 0.07 μmol $m^{-2}$ $s^{-1}$ per 100 cm height of the tide at Eh ≥ 500 mv). During the flood tide, the $CO_2$ flux maintained the largest of the day and almost unchanged with the increase of water level. The average $CO_2$ flux in the flood tide increased with the increase of the redox potential at Eh ≤ 300 mv and 300 mv < Eh < 500 mv, but their linear regressions between the average $CO_2$ flux and the redox potential were different. Compared with the average $CO_2$ flux at Eh ≤ 300 mv and 300 mv < Eh < 500 mv, the average $CO_2$ flux was no longer related to the redox potential but related to temperature at Eh ≥ 500 mv. According to these rules, the daytime $CO_2$ flux can be calculated based on limited measurements well and truly. The fitting straight line equation between the estimated and measured $CO_2$ flux was $y= 0.9353x+0.0872$ ($R^2 = 0.75$, $P < 0.01$).

**Keywords:** intertidal zone, $CO_2$ flux, redox potential

## 1. Introduction

Since global warming become the hot topic, a series of research projects have been trying to give a precise $CO_2$ flux between various ecosystems and the atmosphere. The intertidal zone is the junction of land and sea. It is also a special and important type of wetland. The biogeochemistry environment is complex and unconstant. These properties lead to distinct $CO_2$ exchange mode between intertidal zone and the atmosphere. According to statistics, there are 2.17×104 $km^2$ of the intertidal zone in China (Lei & Zhang, 2005). Although we need a relatively independent $CO_2$ flux research on capacious intertidal zone, the observation on the intertidal zone with static chamber and eddy covariance method was limited (Magenheimer, Moore, Chmura, & Daoust, 1996; Yang et al., 2006; Wang et al., 2007). Mo et al. (2005) estimated the soil respiration based on soil temperature in forest ecosystems; the estimation results were in good agreement with the measured results. Compared with the quantitative estimate of soil respiration in other ecosystems (Davidson, Belk, & Boone, 1998), there has been no similar research on intertidal zone so far. How to give a precise calculation of $CO_2$ flux between intertidal zone and the atmosphere? This paper intends to give a method estimating $CO_2$ flux between intertidal zone and the atmosphere. The method was based on the daytime course of $CO_2$ flux between intertidal sediments and the atmosphere.

## 2. Materials and Methods

### *2.1 Study Site*

This paper selected the Beach (36°05.327'N, 120°27.675'E) of the Shilaoren Scenic Area, Qingdao, China (Figure 1) as the study site. The study site is on the west side of Shilaoren statue. It located between Gaodijiao and Fushanjiao. The length of the beach is about 2.5 kilometers and beach area is about 0.55 $km^2$. The average slope of the beach is 1.5%. The observation site is ~0.7 m above the sea level.

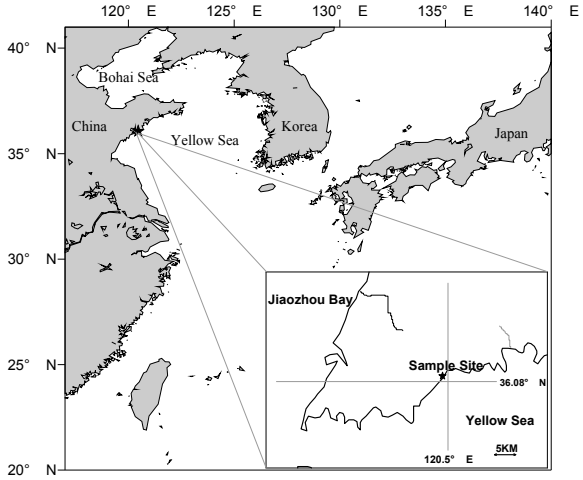


Figure 1. Location of the sample site (★) (Yang et al., 2009; Zhang et al., 2009)

The salinity of the offshore seawater ranged from 26 to 28, because of the impact of the rivers at sourthern Laoshan (about 20 km away). The average temperature of the surface water is 13.5 °C. The observation site is 5 km away from the Maidao Marine Environmental Monitoring Station, Qingdao (www.nmfc.gov.cn). We collected the tide data from this station. The annual mean wave height is 0.7 m. The tide is semi-diurnal. The average high tide is 3.85 m. The average low tide is 1.08 m. This area is north temperate continental monsoon climate. We got the precipitation data from the Coastal Zone Program of the Laoshan Mountain Scenic Area, Qingdao.

We collected sediment samples from the observation site and measured the particle sizes of the sediments by the Cilas940L laser particle size analyzer with the range of 0.3-2000 μm (made in French). The results were shown in Table 1. The particles less than 0.85 mm were 99.99% in the sediments. The largest sediment was less than 8 mm. The median value of the sediment particle sizes was 0.23 mm. And the averages of the gravels were 0.5 mm in diameter.

Table.1 Particle size distribution

| Particle Size | 0.125-0.25 mm | 0.25-0.5 mm | 0.5-0.85 mm |
|---|---|---|---|
| Percentage | 49.67% | 23.26% | 19.55% |

*2.2 Methods*

We used a LI-8100 Automated Soil $CO_2$ Flux System (Licor, Lincoln, Nebraska, USA) to measure $CO_2$ fluxes between the sediment and the atmosphere. The LI-8100 chamber collar is 83.7 $cm^2$. LI-8100 determined the $CO_2$ flux based on the diversification of the $CO_2$ concentration in the chamber. LI-8100 measured $CO_2$ concentration with a non-dispersive infrared detector. The range of the non-dispersive infrared detector was 0 to 3000 ppm. The accuracy was ±1.5%. In half an hour before the beginning of the observation, the collar for the chamber of LI-8100 was inserted into the sediment at 2.4 cm. Each measurement lasted 7 min. The interval between two consecutive measurements was 1min for a full exchange of gases (reference to LI-8100 specification). We took $CO_2$ concentration in the atmosphere 377 ppm and calculated the $CO_2$ flux with the software provided by Licor Corporation.

The LI-8100 system had a temperature probe. The accuracy of the temperature probe was ± 0.5 °C. When observing, the temperature probe was inserted into the sediment at 1 cm. At the same time, the LI-8100 system could also measure the atmospheric $CO_2$ partial pressure at the detector height of 16 cm above the sediment surface.

We used a FJA-16 polarization analyzer (Institute of Soil Science, Nanjing, China) to measure the redox potentials (Eh) of the sediment. The accuracy of FJA-16 was ± 10 mv. When observing, the electrodes of the FJA-16 polarization analyzer together with the chamber collar were inserted into the sediment at 1 cm. Each measurement took 2.5 min.

SPSS 13.0 was used for the statistical analyses of the data.

We selected 19 days from April 24 to July 26, 2006. In these days, there was no rain, the value of wind speed was less than 10 m/s, and there was a tidal cycle during the daytime. We studied the daytime course of the $CO_2$ flux between the sediment and the atmosphere in situ as follows: when the tide ebbed and the site was clear of water, we started the observation; when the tide rose and the site would be submerged we ended the observation; we measured the $CO_2$ flux from the sediment to the atmosphere continuously during the daytime.

## 3. Results and Discussion

### *3.1 The Variation in $CO_2$ Flux During a Daytime Tidal Cycle*

We compared the data from different days with minimum anomaly analysis to conclude the course of $CO_2$ flux in a rounded daytime tidal cycle. The increments of $CO_2$ flux (subtracting the initial $CO_2$ flux from the $CO_2$ flux at a time) were plotted against the height of the tide in Figure 2. Figure 2 shows that the course of the increments of the $CO_2$ flux in the ebb tide was different from the course in the flood tide. In the ebb tide, the increments of the $CO_2$ flux increased as the water level fell and there was a linear relationship between water level and the $CO_2$ flux; in the flood tide, the increments of the $CO_2$ flux reached the maximum and no longer changed as the height of the tide changed. The variation in the increments of $CO_2$ flux determined the variation in $CO_2$ flux. So when the tide was on the ebb, the $CO_2$ flux increased as the water level fell, this increase continued until the tide reached its lowest point (which was also the beginning of the flood tide) and the $CO_2$ flux reached the maximum at the same time. Compared with the variation of the $CO_2$ flux in the ebb tide, the $CO_2$ flux maintained the largest value of the same day with no fundamental changes in the flood tide except slight decline at the end of the flood tide; in addition, the $CO_2$ flux during the flood tide depended on the $CO_2$ flux at the lowest ebb. Thus, the main period of $CO_2$ release in a day was during the flood tide. Because the tide is normal semi- diurnal, $CO_2$ released in the flood tide was about 60% of the $CO_2$ released in the wounded tidal cycle based on the average $CO_2$ flux in the ebb tide and flood tide.

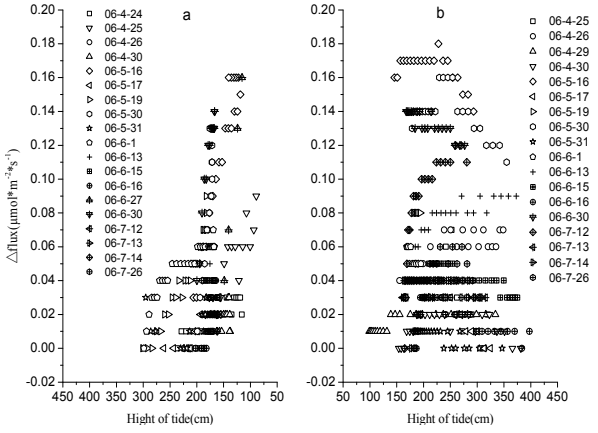


Figure 2. △flux plotted against the height of the tide, (a) for the ebb tide, (b) for the flood tide

### *3.2 The Impact of the Redox Potential on the Variation in $CO_2$ Flux*

The process that sediment releases $CO_2$ to the atmosphere should be similar to soil respiration, which is mainly composed of oxidation of organic matter by soil microbe and plants root respiration, meanwhile, a minute part of which should be attributed to the respiration of soil animals and chemical oxidation of organic matter (Li, Lv, & Yang, 2002). The oxidation of organic matter, the main process releasing $CO_2$, releases less $CO_2$ when the redox potential reduces (Tian, 2005). At different redox potential (Eh), the increments of $CO_2$ flux in the ebb tide were plotted against the height of tide in Figure 3 and the average $CO_2$ flux in the flood tide were plotted against redox potential in Figure 4.

Figure 3 shows that there were different rates of change of the increment in $CO_2$ flux with changes in redox potential in the ebb tide. At Eh ≤ 300 mv, the rate was 0.13 μmol $m^{-2}$ $s^{-1}$ per 100 cm height of the tide, and it reached 0.15 μmol $m^{-2}$ $s^{-1}$ per 100 cm height of the tide at 300 mv < Eh < 500 mv, however, it decreased and was only 0.07 μmol $m^{-2}$ $s^{-1}$ per 100 cm height of the tide at 500 mv ≤ Eh. The variations in the increment of $CO_2$ flux at the tidal height of 0cm were similar to the rates of change of the increment in $CO_2$ flux. The increment of $CO_2$

flux at the tidal height of 0 cm was 0.2654 μmol $m^{-2}$ $s^{-1}$ as the redox potential was lower than 300 mv, and it increased to 0.328 μmol $m^{-2}$ $s^{-1}$ when the redox potential ranged from 300 to 500 mv, however, it decreased to 0.1899 μmol $m^{-2}$ $s^{-1}$ as the redox potential was greater than 500 mv. When the sediment converted from Eh ≤ 300 mv to 300 mv < Eh < 500 mv, the increase in the rate of change of the increment of $CO_2$ flux and the increment of $CO_2$ flux at the tidal height of 0cm should be attributed to the intensification in the oxidation of organic matter. Both the rate of change in the increment of $CO_2$ flux and the increment of $CO_2$ flux at the tidal height of 0cm decreased because of the limitation of organic matter in the sediment when the redox potential was greater than 500 mv.

Redox potential not only affected the variation of $CO_2$ flux in the ebb tide, but also affected average $CO_2$ flux in the flood tide. It is shown in Figure 4 that the average $CO_2$ flux in the flood tide increased as the redox potential rose and there was different relevance between average $CO_2$ flux in the flood tide and redox potential with changes in redox potential. Plotting the average $CO_2$ flux against redox potential gave $R^2$ (0.9167) at Eh ≤ 300 mv, a lower $R^2$ (0.8502) at 300 mv < Eh < 500 mv and there was no significant linear regression between the average $CO_2$ flux and redox potential at 500 mv ≤ Eh. The change in the linear regression between the average $CO_2$ flux and redox potential means that the main controlling factor of $CO_2$ flux in the flood tide had changed when the redox potential rose. In a word, the redox potential was the main controlling factor of $CO_2$ flux in the flood tide when the redox potential was low.

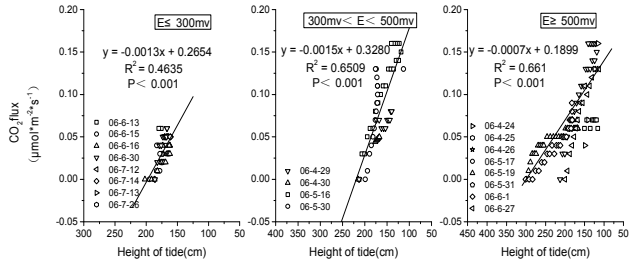


Figure 3. $CO_2$ flux plotted against the height of the tide for different redox potential (Eh) values

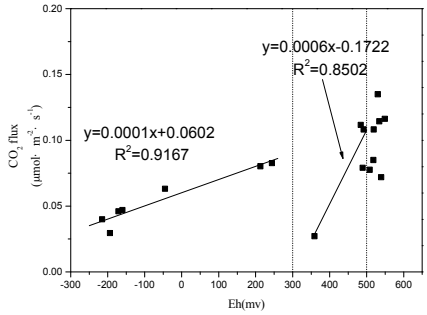


Figure 4. Average $CO_2$ flux at the floodtime plotted against Eh

### *3.3 The Impact of the Temperature on the Variation of $CO_2$ Flux*

Temperature is one of the main influential factors in the past research on soil respiration and $CO_2$ flux between sediment and atmosphere in the coastal salt marsh (Hirota et al., 2007; Blanke, 1996; Luo et al., 2001; Bekku et al., 2003; Smith, 2003; Cao et al., 2004; Wu et al., 2006; Fang, & Moncrieff, 2001). In the ebb tide, however, the correlation coefficient between the temperature and the rates of change of the increment of $CO_2$ flux was -0.093 (p=0.751, n=14), which was lower than the correlation coefficient between the redox potential and the rates of change of the increment of $CO_2$ flux (0.537, p=0.048, n=14). Lower correlation coefficient means that the temperature didn't impact the rates of change of the increment of $CO_2$ flux as significantly as the redox potential in the ebb tide. Although the impact of temperature on $CO_2$ flux is not significant in the ebb tide, the impact of temperature on $CO_2$ flux should be considered in the flood tide, especially 500 mv ≤ Eh. Table 2 shows the Pearson correlation coefficient between the average $CO_2$ flux and temperature in different redox potential in the flood tide. As the redox potential rose, the impact of temperature on the average $CO_2$ flux became more

significant. The correlation coefficient between two variables was 0.366 (p=0.419, n=7) at Eh ≤ 300 mv, and it reached 0.666 (p=0.334, n=4), 0.843 (p=0.017, n=8) at 300 mv < Eh < 500 mv and 500 mv ≤ Eh, respectively. Although the correlation coefficient between temperature and the average $CO_2$ flux was great at 300 mv < Eh < 500 mv, the correlation coefficients (0.922, p=0.078, n=4) between the redox potential and the average $CO_2$ flux was greater. Compared with the redox potential, temperature was not the main influential factor on the average $CO_2$ flux when the redox potential ranged from 300 to 500 mv. Only when the redox potential was greater than 500 mv, temperature was the main controlling factor of the average $CO_2$ flux in the flood tide, and the relationship of two variables was shown in Figure 5.

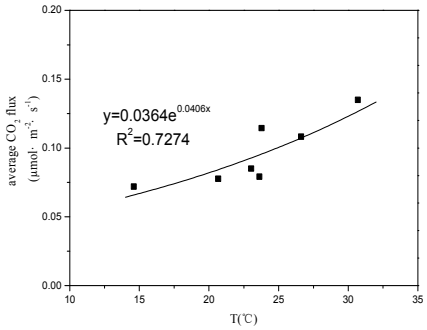


Figure 5. Average $CO_2$ flux at the floodtime plotted against Eh at 500 mv ≤ E

Table 2. Pearson correlation coefficient between daytime average $CO_2$ flux and Temperature in the areas of Figure 3

| | E≤300 mv | 300 mv<E<500 mv | E≥500 mv |
|---|---|---|---|
| Pearson Correlation | 0.366 | 0.666 | 0.843[a] |
| Sig.(2-tailed) | 0.419 | 0.334 | 0.017 |
| n | 7 | 4 | 8 |

a. *P ≤ 0.05*

*3.4 Estimation of $CO_2$ Flux Between the Intertidal Sediment and the Atmosphere*

According to the rule of the variation in the $CO_2$ flux, we can estimate the $CO_2$ flux in the wounded tide cycle based on the $CO_2$ flux in the ebb or flood tide (Figure 6).

$$R_T=R_{ebb}\times t_{ebb}+R_{flood}\times t_{flood} \quad (1)$$

Where $R_T$ is the total $CO_2$ flux from the intertidal sediment to the atmosphere in the daytime, $R_{ebb}$ is the average $CO_2$ flux in the ebb tide, $R_{flood}$ is the average $CO_2$ flux in the flood tide, $t_{ebb}$ is the time span (h) of the ebb tide after the sample site was exposed to the atmosphere and $t_{flood}$ is the time span (h) of the flood tide before the sample was submerged in the water.

There was a linear correlation between $CO_2$ flux and the height of the tide in the ebb tide (Figure 4), so

$$R_{ebb}\approx 0.5(R_{max}+R_{min}) \quad (2)$$

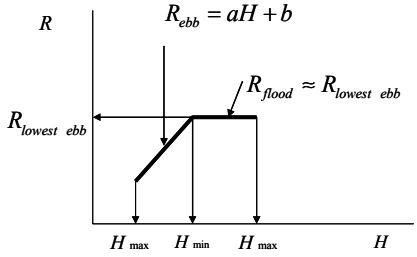


Figure 6. The sketch map for the daytime course of $CO_2$ flux between the sediment and the atmospher, R is the $CO_2$ flux, H is the height of the tide, a and b are the constants

$CO_2$ flux hardly changed in the flood tide (Figure 2), so

$$R_{flood} \approx C \tag{3}$$

(1) If we got some data of $CO_2$ flux in the ebb tide, because R=aH+b in the ebb tide, it should be

$$R_1 = aH_1 + b \tag{4}$$

$$R_{max} = aH_{min} + b \tag{5}$$

$$R_{min} = aH_{max} + b \tag{6}$$

Where $H_1$ is the height of tide (cm) at a point of time in the ebb tide, $R_1$ is the $CO_2$ flux (μmol $m^{-2}$ $s^{-1}$) at $H_1$, $H_{max}$ is the height of tide (cm) when the sample point was submerged in the water, $H_{min}$ is the least height of tide (cm) in the daytime and a is the rate of change of $CO_2$ flux against the height of tide, $R_{max}$ and $R_{min}$ are corresponding $CO_2$ flux at $H_{min}$ and $H_{max}$, a is the rate of change of the increment in $CO_2$ flux; Combining (1), (2), (3), (4), (5) and (6) gives:

$$R_T = 0.5a\ (H_{max} + H_{min} - 2H_1)\ t_{ebb} + R_1 t_{ebb} + C t_{flood} \tag{7}$$

Where C is the average $CO_2$ flux in the flood tide.

(2) If we got some data of $CO_2$ flux in the flood tide, then

$$C = R_2 = R_{max} \tag{8}$$

Combining (2), (3), (5), (6) and (8) gives

$$R_T = 0.5a\ (H_{max} - H_{min})\ t_{ebb} + R_2\ (t_{ebb} + t_{flood}) \tag{9}$$

Where $R_2$ is the $CO_2$ flux (μmol $m^{-2}$ $s^{-1}$) at a point of time in the flood tide.

Figures 3, 4 and 5 shows that

$$a = \begin{cases} -0.0013 & Eh \le 300mv \\ -0.0015 & 300 < Eh < 500mv \\ -0.0007 & Eh \ge 500mv \end{cases}$$

$$C = \begin{cases} 0.0001Eh + 0.0602 & Eh \le 300mv \\ 0.0006Eh - 0.1722 & 300 < Eh < 500mv \\ 0.0364e^{0.0406T} & Eh \ge 500mv \end{cases}$$

Combining equations on a and C,

$$R_T = \begin{cases} 0.5a(H_{max} + H_{min} - 2H_1)\, t_{ebb} + R_1 t_{ebb} + C t_{flood} \\ 0.5a(H_{max} - H_{min})\, t_{ebb} + R_2 (t_{ebb} + t_{flood}) \end{cases}$$

$$a = \begin{cases} -0.0013 & Eh \le 300mv \\ -0.0015 & 300 < Eh < 500mv \\ -0.0007 & Eh \ge 500mv \end{cases}$$

$$C = \begin{cases} 0.0001Eh + 0.0602 & Eh \le 300mv \\ 0.0006Eh - 0.1722 & 300 < Eh < 500mv \\ 0.0364e^{0.0406T} & Eh \ge 500mv \end{cases}$$

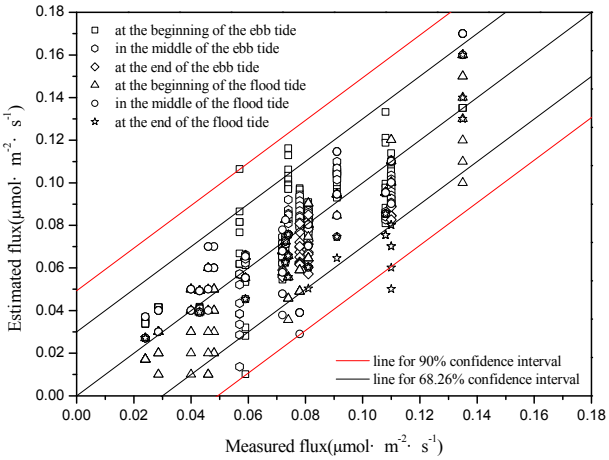


Figure 7. Relationship between measured and estimated average $CO_2$ flux

Above equation is not a simple linear fitting equation, but a composite equation based on the rule of the variation in the $CO_2$ flux. We estimated the $CO_2$ flux with the equation and plotted the estimations against the measured $CO_2$ fluxes in Figure 7 to test the reliability of the equation. Figure 7 shows that the estimated fluxes were all but in the 90% confidence interval and most of the estimated fluxes were in the 68.26% confidence interval. On the other hand, the linear regression between the estimated and measured fluxes was $y = 0.9353x+0.0872$ ($R^2 = 0.75$). Thus it can be seen that the Equations (7) and (9) could well estimate the daytime average $CO_2$ flux.

## 4. Conclusions

Based on the analysis performed, the following conclusion can be shown:

(1) The $CO_2$ flux increased as the water level fell during the ebb tide, while it maintained the largest of the same day with no fundamental changes during the flood tide.

(2) During the ebb tide, the $CO_2$ flux rose as the tide ebbed and its rate of change was different when the redox potential changed. The rate of change of the $CO_2$ flux was 0.13 μmol $m^{-2}$ $s^{-1}$ per 100 cm height of the tide at Eh ≤ 300 mv, while it was 0.15 μmol $m^{-2}$ $s^{-1}$ per 100 cm height of the tide at 300 mv < Eh < 500 mv and 0.07 μmol $m^{-2}$ $s^{-1}$ per 100 cm height of the tide at Eh ≥ 500 mv respectively.

(3) The average $CO_2$ flux in the flood tide increased with the increase of the redox potential at Eh ≤ 300 mv and 300 mv < Eh < 500 mv, while it was no longer related to the redox potential but related to temperature at Eh ≥ 500 mv.

(4) According to the rules on the variation in $CO_2$ flux, the daytime $CO_2$ flux can be calculated based on limited measurements well and truly. The fitting straight line equation between the estimated and measured $CO_2$ flux was $y = 0.9353x+0.0872$ ($R^2 = 0.75$, $P < 0.01$).

## Acknowledgments

The authors would like to show their gratitude to National Science Foundation of China (Project No.: 40476063), National Basic Research Program of China (Project No.: 2002CB412504), Youth Foundation of North China Sea Branch of State Oceanic Administration (Project No.: 2012A02) and Open Foundation of MOIDAT (Project No.: 201307). The authors thank Dr. J. Zhang for her suggestions on the manuscript.

## References

Bekku, Y. S., Nakatsubo, T., Kume, A., Adachi, M., & Koizumi, H. (2003). Effect of warming on the temperature dependence of soil respiration rate in arctic, temperate and tropical soils. *Appl. Soil Ecol., 22*(3), 205-210. http://dx.doi.org/10.1016/S0929-1393(02)00158-0

Blanke, M. M. (1996). Soil respiration in an apple orchard. *Environ. Exp. Bot, 36*(3), 339-341. http://dx.doi.org/10.1016/0098-8472(96)01003-9

Cao, G., Tang, Y., Mo, W., Wang, Y., Li, Y., & Zhao, X. (2004). Grazing intensity alters soil respiration in an alpine meadow on the Tibetan plateau. *Soil Bio. Biochem., 36*(2), 237-243. http://dx.doi.org/10.1016/j.soilbio.2003.09.010

Davidson, E. A., Belk, E., & Boone, R. D. (1998). Soil water content and temperature as independent or confound factors controlling soil respiration in a temperate mixed hardwood forest. *Global Change Biology, 4*, 217-227. http://dx.doi.org/10.1046/j.1365-2486.1998.00128.x

Fang, C., & Moncrieff, J. B. (2001). The dependence of soil $CO_2$ efflux on temperature. *Soil Biology and Biochemistry, 33*(2), 155-165. http://dx.doi.org/10.1016/S0038-0717(00)00125-5

Hirota, M., Senga, Y., Seike, Y., Nohara, S., & Kunii, H. (2007). Fluxes of carbon dioxide, methane and nitrous oxide in two contrastive fringing zones of coastal lagoon, Lake Nakaumi, Japan. *Chemosphere, 68*(3), 597-603. http://dx.doi.org/10.1016/j.chemosphere.2007.01.002

Lei, K., & Zhang, M. X. (2005). The wetland resources in China and the conservation advices. *Wetland Scinece, 3*(2), 81-86.

Li, Z. F., Lv, X. G., & Yang, Q. (2002). A review on wetland soil $CO_2$ flux. *Chinese Journal of Ecology, 21*(6), 47-50.

Luo, Y., Wan, S., Hui, D., & Wallace, L. L. (2001). Acclimatization of soil respiration to warming in a tall grass prairie. *Nature (London, U. K.), 413*(6856), 622-625. http://dx.doi.org/10.1038/35098065

Magenheimer, J. F., Moore, T. R., Chmura, G. L., & Daoust, R. J. (1996). Methane and carbon dioxide flux from a macrotidal salt marsh, Bay of Fundy, New Brunswick. *Estuaries, 19*(1), 139-145. http://dx.doi.org/10.2307/1352658

Mo, W., Lee, M. S., Uchida, M., Inatomi, M., Saigusa, N., Mariko, S., & Koizumi, H. (2005). Seasonal and annual variations in soil respiration in a cool-temperate deciduous broad-leaved forest in Japan. *Agr. Forest Meteorol., 134*(1-4), 81-94. http://dx.doi.org/10.1016/j.agrformet.2005.08.015

Smith, V. R. (2003). Soil respiration and its determinants on a sub-Antarctic island. *Soil Bio. Biochem., 35*(1), 77-91. http://dx.doi.org/10.1016/S0038-0717(02)00240-7

Tian, Y. B. (2005). Advance in research on carbon cycling in wetland soil. *Journal of Yangtze University, 2*(8), 1-5.

Wang, D. Q., Chen, Z. L., Wang, J., Xu, S. Y., Yang, H. X., Chen, H., & Yang, L. Y. (2007). Fluxes of $CH_4$, $CO_2$ and $N_2O$ from Yangtze estuary intertidal flat in summer season. *Geochimica, 36*(1), 78-88, 2007.

Wu, J., Guan, D., Wang, M., Pei, T., Han, S., & Jin, C. (2006). Year-round soil and ecosystem respiration in a temperate broad-leaved Korean Pine forest. *Forest Ecol. Manag., 223*(1-3), 35-44. http://dx.doi.org/10.1016/j.foreco.2005.10.055

Yang, H. X., Wang, D. Q., Chen, Z. L., Chen, H., Wang, J., Xu, S. Y., & Yang, L. Y. (2006). Characteristics of carbon fluxes through intertidal flat wetland-atmosphere interface of Yangtze estuary. *Acta Scientiae Circumstantiae, 26*(4), 667-673.

Yang, P. J., & Zhang, L. J. (2009). Sediment temperature and redox potential as confound factors controlling $CO_2$ flux between sediment and the atmosphere in an intertidal zone. *3rd International Conference on Bioinformatics and Biomedical Engineering, iCBBE*.

Zhang, L. J., & Yang, P. J. (2009). Main factors impacting the $CO_2$ flux between sediment and the atmosphere in an intertidal zone, Qingdao. *3rd International Conference on Bioinformatics and Biomedical Engineering, ICBBE*.